Chitosan-capped silver nanoparticles: A comprehensive study of polymer molecular weight effect on the reaction kinetic, physicochemical properties, and synergetic antibacterial potential

Viktoryia Kulikouskaya, Kseniya Hileuskaya, Aliaksandr Kraskouski, Irina Kozerozhets, Elena Stepanova, Ivan Kuzminski, Lijun You, Vladimir Agabekov
First published: 04 February 2022

https://doi.org/10.1002/pls2.10069

Abstract

The search for novel efficient antibacterial agents is attracting a great attention due to the unregulated use of common antibiotics and development of multidrug-resistant bacteria strains. This paper proposes an eco-friendly approach to obtain stable chitosan-capped silver nanoparticles with controlled physicochemical and biological properties using reducing and stabilizing capacity of chitosan. The study of the influence of chitosan characteristics on the kinetic of Ag^+ reduction showed that an increase in polysaccharide molecular weight led to a decrease in their reducing ability. The synthesized silver nanoparticles were characterized by UV and FTIR spectroscopy, TEM, XRD, DLS. The relationships between physicochemical characteristics of the formed silver nanoparticles and the type of used chitosan, as well as synthesis temperature, were determined. It has been demonstrated that spherically-shaped (13–27 nm) and positively-charged (zeta-potential 26.1–29.5 mV) silver nanoparticles with a single symmetric SPR band at 408–418 nm are stable during 6 months in a colloidal form, and can be produced with the assistance of low-molecular weight chitosan (20–30 kDa) at 95°C. The synthesized silver nanoparticles enhanced the antibacterial activity of kanamycin and ampicillin against both gram-negative and gram-positive bacteria. These results revealed the prospects for the application of chitosan-capped silver nanoparticles to create new effective antibacterial systems (gels, films, etc).

1 INTRODUCTION

Infections caused by pathogenic bacteria are still one of the serious health and economic problems, because unregulated use of antibiotics leads to the development of multidrug-resistant bacteria strains and decreases in antibiotic efficiency.[1, 2] Therefore, it has become necessary to search for alternative and more efficient antibacterial agents, as well as approaches to overcome the problem of bacterial resistance.[1-5] Currently, inorganic nanoparticles are under extensive investigation as one of the strong alternatives to various antibacterial agents, as well as for other biomedical applications.[1, 2, 6-8] The main benefits of such nanoparticles include their high efficiency against a broad range of microbes and parasites, as well as the ability to disrupt microbial biofilms.[1, 2, 6, 7] The particular interest in silver nanoparticles for biomedical applications is mainly due to their excellent antimicrobial activity, limited anti-pathogenic resistance and impressive efficiency against multidrug-resistant microorganisms.[2, 7, 9] It should be noted that the exact mechanism of antibacterial action of Ag nanoparticles (NPs) on bacterial cells has not been entirely clarified yet. However, several concepts have been proposed to explain the mechanism of their antibacterial action: (1) destruction of the membrane and leakage of cellular contents, (2) generation of the reactive oxygen species, (3) destruction of the DNA structure, (4) inactivation of enzymes.[2, 9-13] It is suggested that the primary mechanism of action of silver nanoparticles is interaction with cell membrane, causing an increase in its permeability and loss of integrity. The wide application of silver nanoparticles in medicine is hindered by the low stability of bare nanoparticles and high-level cytotoxicity.[7] In this regard, a number of studies are devoted to the search for approaches to reduce the toxicity of silver nanoparticles. Some works have reported that the modification of Ag nanoparticles with biopolymer coating can affect their bioavailability and toxicity.[7, 14-16] It is noteworthy, that besides biomedical applications, Ag NPs have also received attention in other cutting-edge fields, including diagnostic, water treatment, optical sensors, etc.[17-20]

Currently, an in-depth study was conducted on synthesis of eco-friendly silver nanoparticles using plant extracts and natural compounds (polysaccharides, polyphenols, etc.) as reducing and/or capping agents.[14, 17, 21-31] The main benefits of this green chemistry approach are the absence of toxic reducers and organic solvents in the reaction media, the use of biopolymer both as a reducing agent and a stabilizer for the formed Ag NPs. From the point of view of eco-friendly reducing and stabilizing agents, chitosan deserves special attention in the synthesis of Ag NPs. Chitosan is a linear polycationic polysaccharide, composed of randomly distributed *β*-(1 → 4)-linked D-glucosamine (deacetylated unit) and *N*-acetyl-D-glucosamine (acetylated unit). Chitosan is obtained by deacetylation of chitin, which is the second most ubiquitous natural polysaccharide after cellulose on Earth. Chitin is widely distributed in crustaceans, insects, fungi, and yeast. Chitosan as biopolymer possesses huge advantages over petroleum-based synthetic polymers by means of cost effectiveness, eco-friendliness, and non-toxicity.[32, 33] It should be noted that most of the naturally occurring polysaccharides (cellulose, alginic acid, pectin, carrageenan, etc.) are neutral or acidic in nature. Chitosan, in turn, is a polycation containing amino-groups. The base nature of chitosan macromolecules determines its unique properties including chelatation of metal ions, antimicrobial activity, mucoadhesive ability, etc. Thus, chitosan is a promising biocompatible and biodegradable polymer for biomedical purpose with an inherent antimicrobial activity and a mucoadhesive behavior. The synthesis of Ag NPs under the action of chitosan has also a number of advantages. Firstly, chitosan is able to reduce Ag^{+} to Ag^{0} and simultaneously stabilize the forming Ag NPs due to the formation of a biopolymer shell on their surface. It is known[34] that polymers with functional groups, which are able to interact with metal ions, and structural elements, which can provide steric or Coulomb stabilization of the

formed Ag nanoparticles colloids, are the best stabilizers. Due to the presence of amino groups, chitosan macromolecules can interact with silver cations and stabilize Ag NPs. The stabilization process can be explained by the formation of hydrogen, electrostatic, Van-der-Waals or other bonds between the surface of nanoparticles and chitosan macromolecules. It is noteworthy, that chitosan-stabilized silver nanoparticles (CS-Ag NPs) can exhibit the properties inherent to each of the components, including possible appearance of a synergistic antibacterial action. The antibacterial action of chitosan is associated with its ability to bind to the negatively charged bacterial surface which causes the destruction of cell membrane and alters its permeability.[35] It should be noted, that in multiple toxicity study Asghar and co-authors demonstrated a low cytotoxicity of chitosan-coated silver nanoparticles compared to Ag nanoparticles alone.[16] All these benefits have led to a large number of studies on the preparation of chitosan-stabilized silver nanoparticles.[31, 36-41] Unfortunately, most publications mainly focus on the characterization of the obtained Ag NPs without taking into account the characteristics of the used chitosan. At the same time, chitosan is isolated from natural sources (the exoskeleton of crustaceans and cell walls of fungi), therefore, its characteristics (molecular-weight distributions, acetylation degree, etc.) strongly depend on the origin source and method of manufacture and can affect biopolymer reducing and stabilization ability. Thus, the results obtained for a certain type of chitosan on the synthesis of Ag NPs cannot be identical to the ability of another chitosan sample (e.g., isolated from other sources and/or under differ conditions) to produce the same nanoparticles. Pursuant thereto, it is important to carry out a comprehensive study of the influence of chitosan molecular weight on its ability to produce Ag NPs, as well as their physicochemical characteristics and stability upon storage.

In this work we carried out comprehensive research on the influence of chitosan molecular weight and synthesis temperature on the kinetic of Ag^+ reduction, as well as physicochemical properties (size distribution, zeta potential, aggregative stability) of the formed chitosan-capped silver nanoparticles. We have established a key chitosan characteristic that determines the possibility of obtaining chitosan-capped silver nanoparticles which have a long-term stability in a colloidal form upon storage. The potential of the synthesized chitosan-capped silver nanoparticles to increase the activity of common antibiotics have also been studied in details.

2 MATERIALS AND METHODS

Synthesis of chitosan-capped Ag nanoparticles (CS-Ag NPs)

To synthesize silver nanoparticles stabilized by chitosan, 1 ml of the freshly prepared aqueous solution of $AgNO_3$ (20 mM) was added to 10 ml of chitosan solution (10 mg/ml) in 2% acetic acid. Then the reaction mixture was placed in a water bath (LOIP LB-160, Russia) followed by thermostating at 60, 80, or 95°C. The synthesized nanoparticles were purified from the residues of the reaction mixture by dialysis overnight (16 h, Dialysis tubing cellulose membrane Sigma D9652, molecular weight cut-off = 14,000) against distilled water.

UV–Vis absorption spectra of the reaction mixture were recorded during the synthesis using Solar CM 2203 (Belarus) spectrofluorimeter in the range of 350–650 nm. Chitosan with different molecular weight (20 kDa (CS20, Glentham Life Sciences); 30 kDa (CS30, Glentham Life Sciences); 340 kDa (CS340, SigmaAldrich); 800 kDa (CS800, SigmaAldrich)) was used to synthesize silver nanoparticles.

Atomic absorption spectroscopy

The amount of the unreacted Ag^+ after synthesis or released Ag^+ during storage was measured by atomic absorption spectroscopy (AAS). The samples of CS-Ag NPs were placed in a dialysis tubing cellulose membrane (D9652, Sigma). Then the dialysis was carried out three times against distilled water and water samples were collected. The concentration of Ag^+ in dialysis water was determined using High-Resolution Continuum Source Flame Atomic Absorption Spectrometer ContrAA 300 (Analytik Jena AG, Jena, Germany), equipped with a xenon short-arc lamp. Acetylene flame (C_2H_2) was used for atomization of Ag^+.

Characterization of CS-Ag NPs

An average hydrodynamic diameter and polydispersity index (PdI) of the CS-Ag NPs were measured by dynamic light scattering technique using Zetasizer Nano-ZS analyzer (Malvern, UK). The value of the zeta-potential was calculated from the Smoluchowski equation on the basis of electrophoretic mobility data obtained by Zetasizer Nano-ZS analyzer (Malvern, UK).

Shape and size of CS-Ag NPs were evaluated by transmission electron microscopy (TEM) using JEOL-LEM-1400 unit (Jeol Ltd., Tokyo, Japan). TEM samples were prepared by dropping the colloidal solution onto a copper grid and drying in the air.

Fourier transform infrared (FTIR) spectroscopic analysis was performed in the range from 400 to 4000 cm^{-1}, using Tensor-27 spectrophotometer (BRUKER, Germany). Data collection was performed with a 4 cm^{-1} spectral resolution and 32 scans. Samples for measurement were lyophilized and pressed in KBr pellets.

X-ray diffraction analysis was carried out on a D8 ADVANCE ECO diffractometer (Bruker, Germany) using CuKα radiation (λ = 1.5406 Å) at 2θ = 10°–60° with a step size of 0.0133°. In order to identify the phases and study the crystalline structure, the software BrukerAXSDIFFRAC.EVAv.4.2 and the international ICDD PDF-2 database were used.

Determination of antibacterial activity

Antibacterial activity of CS-Ag NPs was evaluated by well diffusion method using strains of gram-positive *Staphylococcus aureus* (KMIEV B161) and gram-negative *Escherichia coli* (KMIEV B88) bacteria grown on meat peptone agar without antibiotics.

The studied bacterial culture (200 million cells/ml) was inoculated with a lawn on meat peptone agar in a Petri dish. Then kanamycin (30 μg) and ampicillin (10 μg) standard discs (NICF, Russia) were placed on the seeded surface. To determine their combined effect with the synthesized nanocomposites, each standard paper disc was impregnated with 30 μl of CS-Ag solution. Antibiotic disks impregnated with 30 μl of distilled water or chitosan solution were used as control samples. After incubation at 37°C for 20 h, the zone of bacterial growth inhibition was measured.

3 RESULTS AND DISCUSSION

Effect of chitosan molecular weight on the kinetic of $AgNO_3$ reduction

Silver nanoparticles stabilized by chitosan macromolecules were synthesized by green chemistry approach via chemical reduction of Ag^+ cations with polysaccharide. In this reaction, chitosan macromolecules act both as a reducing and stabilizing (capping) agent. It is assumed that the reduction of silver cations by the chitosan macromolecules includes several stages. It is well known that NH_2-groups in chitosan macromolecules possess strong complexation abilities with metal ions. Therefore, at the first stage silver cations react with chitosan amino groups, fixed on polymer chains.[42] Then silver cations are reduced by the functional groups of chitosan. According to the References [42, 43], in this reduction reaction primary and secondary alcohol are oxidized to aldehyde and ketone respectively. The authors[43] also suggest that the glycosidic bond can participate in the reduction of Ag^+, leading to the formation of a ketone at C_4 or an ester at C_1 atoms of the glycosidic ring.

To study the influence of polymer characteristics on the ability to produce Ag NPs, chitosan with molecular weight of 20 to 800 kDa has been chosen. It should be noted that a single surface plasmon resonance (SPR) band of Ag NPs has not been registered for samples obtained upon Ag^+ reduction by chitosan at room temperature (Figure S1). Apparently, all spectra contain a combination of different spectrally overlapped SPR bands, indicating that Ag NPs are varied in size and shape. Moreover, the adsorption spectra of the samples obtained with the assistance of low-molecular weight chitosan exhibited a peak with a maximum at 360 (A = 0.11) and 373 (A = 0.12) nm for CS20 and CS30 respectively (Figure S1). This band can be associated with the absorption by the particles of quasi-metallic silver.[44] Increase in chitosan molecular weight led to the formation of burgundy-brown solutions with high absorbance (Figure S1). However, the characteristic absorption bands of colloidal silver can be distinguished at 387 (A = 1.82) and 480 (A = 1.99) nm in the spectra of Ag-CS800 (Figure S1). Therefore, in order to obtain hydrosols with fine Ag NPs, the effect of an increase in reaction temperature on their formation has been studied.

The role of chitosan molecular weight in the reduction of $AgNO_3$ during Ag NPs synthesis at different reaction temperature was firstly evaluated using UV–Vis observations (Figure 1). In the case of low molecular weight chitosan (20 and 30 kDa), the color of reaction mixtures turned reddish yellow even at 60°C indicating the formation of Ag NPs (Figure S2). The increase in the reaction temperature up to 95°C led to a significant enhancement in the intensity of SPR band at 418 and 408 nm for CS20 and CS30, respectively (Figure 1A,B). Thus, this data indicated the increase in Ag NPs content upon increasing reaction temperature keeping other conditions unchanged. It should be noted that the reduction process proceeded most intensively under the action of CS20. So, the intensity of SPR band was equal to 0.797 for a 10-fold diluted CS20-Ag solution compared to the value of 0.880 for the undiluted CS30-Ag (Figure 1A,B). According to the UV–Vis data (Figure 1C,D), the formation of Ag NPs under the action of medium weight chitosan took place only at high-reaction temperature (95°C). When CS340 and CS800 were used to produce silver nanoparticles, broad spectra with a maximum at 405–408 nm were observed indicating a broad nanoparticles distribution (Figure 1C,D). No clear SPR band was detected for the samples produced with the assistance of CS340 and CS800 at 65 and 80°C (Figure 1C,D), therefore their burgundy-brown color (Figure S2) could be associated with the formation of other silver species (i.e., Ag_2O, AgO, etc.). Thus, the obtained data displayed that the increase in chitosan molecular weight resulted in the decrease in their reduction ability towards silver cations.

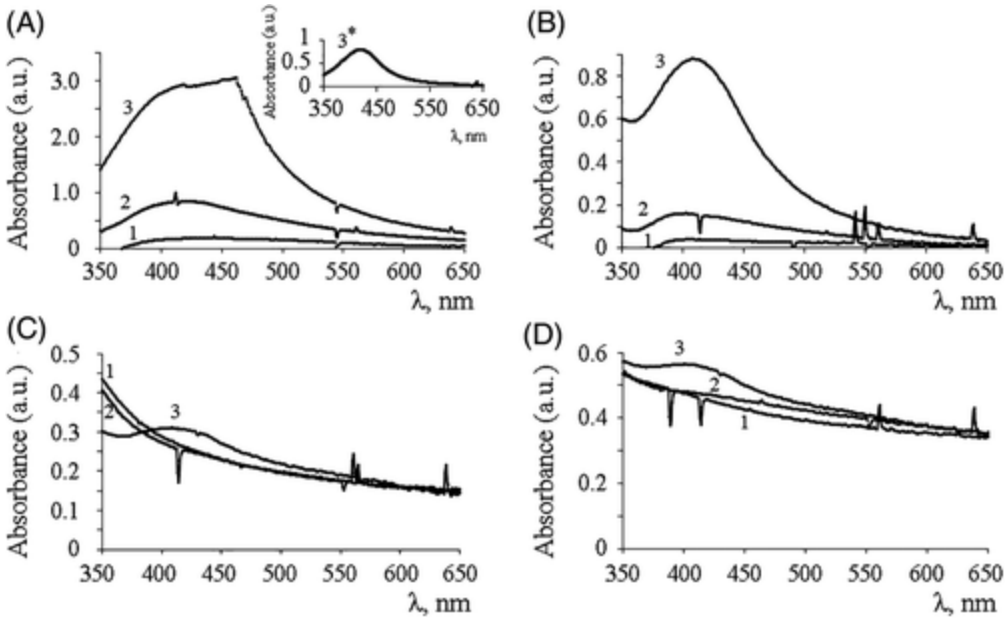

FIGURE 1

Open in figure viewerPowerPoint

UV–Vis spectra of the reaction mixture after 6 h at 60°C (1), 80°C (2), and 95°C (3): (A) CS20, (B) CS30, (C) CS340, (D) CS800

For further application of the obtained CS-Ag NPs as antibacterial agents, it is important to evaluate the total amount of silver in nanocomposites. Unfortunately, a lot of publications on the antibacterial properties of Ag NPs neglected the conversion degree and the amount of the unreacted Ag^+ disposed during purification of the product.[25, 30, 37, 45-48] Therefore, we have evaluated the amount of free unreacting Ag^+ in dialysis media after synthesis using AAS. According to the AAS data, the highest conversion (~60%) was achieved for CS20. The lower conversion degree (16%) was found for CS30. Surprisingly, that the detected amount of Ag^+ cations in the dialysis media for CS340-Ag and CS800-Ag samples was only 80% and 62%, respectively. At the same time, according to UV–Vis data, these samples were characterized by low-intensity SPR bands (Figure 1C,D). Apparently, these samples contained a significant amount of other silver species.

Next, the kinetic parameters of the Ag^+ reduction by chitosan macromolecules were evaluated for CS20 and CS30. For kinetic characterization of CS-Ag NPs formation, the absorbance at SPR band maximum was plotted versus reaction time (Figure 2). This approach has also been previously used by several authors[49, 50] for the analysis of the kinetic regularities of Ag NPs formation. As can be seen in Figure 2, the dependence of the absorbance at λ_{max} on time was fitted reasonably well (*R*-squared more than 0.96) by a linear approximation regardless of the reaction temperature and chitosan molecular weight. According to the chemical kinetics, this dependence corresponds to a zero-order reaction. It was unexpected, because the authors[21, 37] have earlier reported that the reduction of silver cations by biopolymers (medium weight chitosan, lignin) obeys a pseudo-first order. At the same time, it is well known that zero-order reaction means that the rate of reaction is independent of the reactant concentration. This type of reaction occurs when a material that is required for the reaction to proceed is saturated by the reactants. Zero-order can be observed for heterogeneous reactions if the rate of reagent diffusion to the interface is less than the rate of their chemical transformation. In our case, at the first stage the coordination of Ag^+ to electron pairs situated on nitrogen of NH_2-groups of chitosan could take place.[51] Moreover, in the studied conditions, there was a large excess of chitosan in the reaction medium, therefore, regardless of whether the concentration of chitosan or

silver nitrate increases, all silver cations can be bound into coordination complexes. Therefore, it can be assumed that in reaction mixture all silver cations formed coordination complexes with chitosan macromolecules and the rate of silver nanoparticles formation did not depend on the concentration of the reagents. It is worth noting that authors[49] observed the similar data. They showed that in the presence of chitosan in the reaction media, the reduction of Ag^+ by galactose carried out very slowly and the "absorbance-time" dependence of Ag nanoparticles formation was also a straight line.[49] As the reaction temperature increased from 60 to 95°C, the rate constant for CS20 enhanced by an almost one order of magnitude: from 0.0019 to 0.012. The reaction rate in the case of CS30 was slower compared to CS20 and the rate constant enhanced from 0.0001 to 0.002 with increasing temperature from 60 to 95°C. The activation energy of the Ag nanoparticles formation was calculated according to the Arrhenius equation (Figure 3). The calculated activation energy was equal to 60 and 57 kJ/mol for CS20 and CS30, respectively. These data are in good agreement with the previously reported values of activation energy for Ag nanoparticles formation.[50]

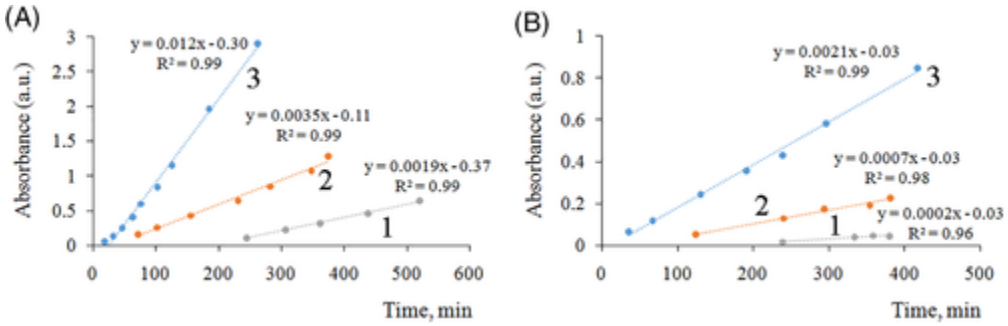

FIGURE 2

Open in figure viewerPowerPoint

The dependence of absorbance at λ_{max} from time upon CS20-Ag (A) and CS30-Ag (B) formation at 60°C (1), 80°C (2), and 95°C (3)

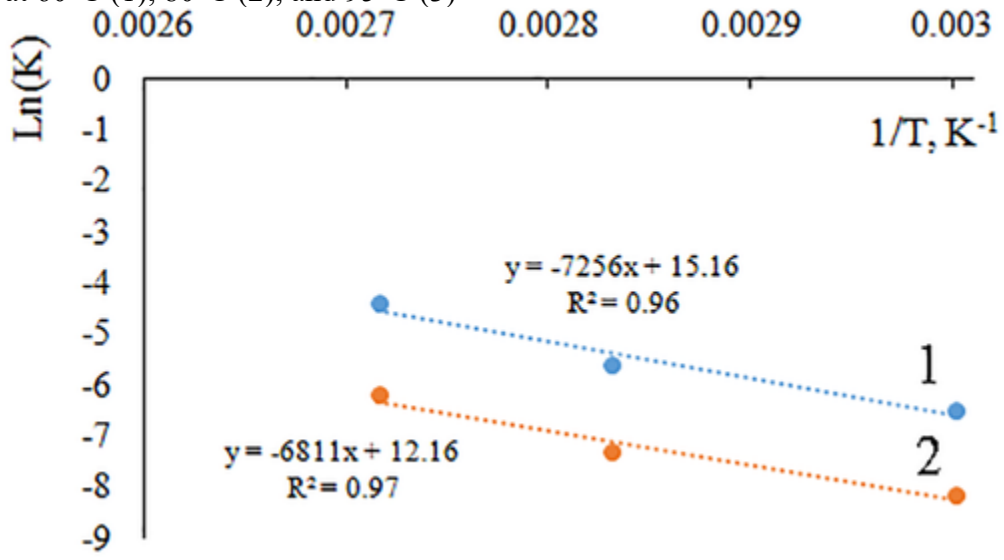

FIGURE 3

Open in figure viewerPowerPoint

Arrhenius plots of ln(K) versus 1/T: 1—CS20-Ag, 2—CS30-Ag

The dimensional analysis of the prepared CS-Ag NPs was carried out using transmission electron microscopy (TEM) and dynamic light scattering (DLS). The TEM images revealed the fabrication of spherically shaped nanoparticles in all samples (Figure 4). CS20-Ag nanoparticles were the most polydisperse among the synthesized samples: the size distribution was ranging

from 5 to 65 nm (Figure 4A). CS30 allowed to produce smaller particles with a mean diameter of 13 ± 5 nm (Figure 4B, Table 1). The mean diameters of particles, formed under the action of CS340 and CS800, were 13 ± 3 and 13 ± 6 nm, respectively (Table 1). It is worth noting that the core-shell structure of the obtained nanocomposites was also confirmed by TEM: for CS20-Ag and CS30-Ag shell size was about 3–5 nm (Figure 4A,B).

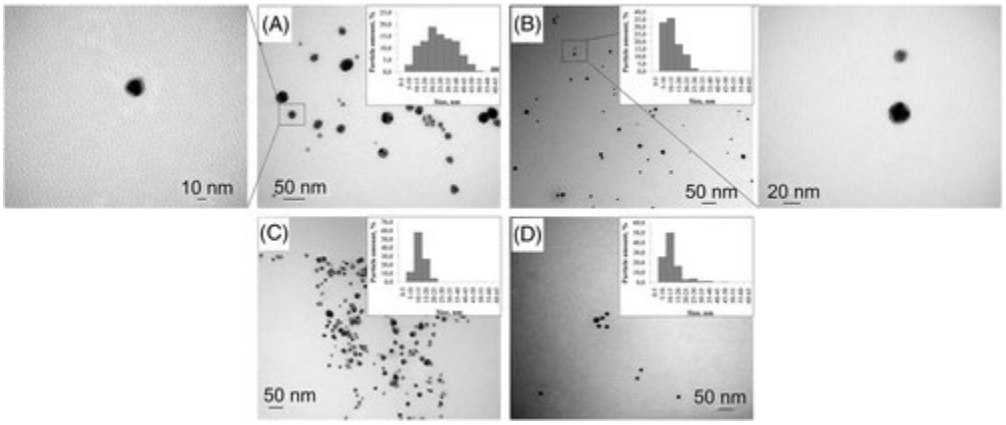

FIGURE 4
Open in figure viewerPowerPoint
TEM images and the size distribution (insets) of CS20-Ag (A), CS30-Ag (B), CS340-Ag (C), and CS800-Ag (D) NPs

TABLE 1. Characteristics of chitosan-capped silver nanoparticles

Chitosan	d_{TEM}, nm	d_{mean} (DSL), nm	PdI	Zeta potential, mV	Yield, %
CS20	27 ± 11	115	0.373	26.7 ± 9.3	82.6 ± 0.9
CS30	13 ± 5	230	0.333	26.6 ± 5.9	90.2 ± 2.4
CS340	13 ± 3	1780	0.225	29.5 ± 5.8	85.9 ± 4.2
CS800	13 ± 6	2430	0.344	26.1 ± 6.9	85.2 ± 3.8

The DLS analysis reveals the hydrodynamic diameter representing the size of solvent associated nanoparticles and provides information about the size of CS-Ag NPs with a hydrated polymer shell. It has been determined that the hydrodynamic diameter of the particles strongly depended on the molecular weight of the used chitosan (Table 1). Increase in chitosan molecular weight from 20 to 800 kDa led to significant enhance their hydrodynamic diameter more than 10 times: from 115 to 2430 nm indicating the formation of thick hydrated biopolymer coatings on the surface of Ag NPs (Table 1).

The observed difference between the TEM and DLS data is due to the fact that the hydrodynamic diameter includes both the core size and the stabilizing polymer shell swollen in an aqueous medium. In this regard, it is reasonable that an increase in the molecular weight of the polymer in the shell led to an increase in the hydrodynamic diameter of the obtained particles. The DSL data also revealed that the formed nanoparticles were fairly uniform: the polydispersity index (PdI) did not exceed 0.4 (Table 1). Thus, based on the TEM and DLS data, it can be concluded that increase in chitosan molecular weight did not lead to the significant change in the size of inorganic core, but resulted in the formation of the thick biopolymer shell on its surface.

The mean zeta-potential value of CS-Ag NPs and their yield were additionally presented in Table 1. Results showed that, regardless of the molecular weight of chitosan, the value of zeta-potential for nanoparticles was more than 25 mV (Table 1), which indicated high-aggregative stability due to strong repulsive forces among the nanoparticles. It has been calculated that the yield of CS-Ag NPs was 82%–90% (Table 1). It means that during synthesis of silver nanoparticles scission of chitosan chains could take place, which led to a decrease in its molecular weight and a subsequent removal of the low molecular weight fraction during dialysis. It is well known that upon storage of acetic acid solutions of chitosan, the degradation of chitosan chain occurs at elevated temperatures.[52, 53] It should be pointed out that the obtained data can also confirm the hypothesis of Carapeto and co-authors[43] about the contribution of the glycosidic bond in the reduction of silver cations.

The X-ray diffraction (XRD) analysis was used to verify the presence of Ag^0 in the synthesized nanocomposites. The XRD pattern of CS20-Ag NPs demonstrated the small characteristic peak of the crystalline phase and the amorphous halo (Figure 5). Presence of the Bragg reflections with 2θ values of 38.2^0 and 44.3^0, corresponding to (111) and (200) planes for face-centered-cubic lattice of Ag (ICDD PDF-2 card no: 00-004-0783), have indicated that pure crystalline silver could be produced with the assistance of low molecular weight chitosan. The peaks of crystalline silver were almost indistinguishable on the XRD patterns of CS30-Ag and CS340-Ag, which was due to very low content of silver nanoparticles in these nanocomposites and a large share of chitosan. It should be noted that XRD patterns of CS30-Ag and CS340-Ag nanocomposites exhibitied characteristic peaks at $2\theta = 14.1°$ and 17.1° which are attributed to anhydrous crystal lattice in chitosan.[54] In the XRD pattern of CS800-Ag, there were some new peaks at $2\theta = 32.1°$ and 46.2° (Figure 5) associated with the crystal phase of (111) and (211) of Ag_2O (ICDD PDF-2 card no: 01-078-5868).[55] These data are in good agreement with AAS and UV–Vis results which supposed the formation of other silver species in CS800-Ag samples except for Ag nanoparticles.

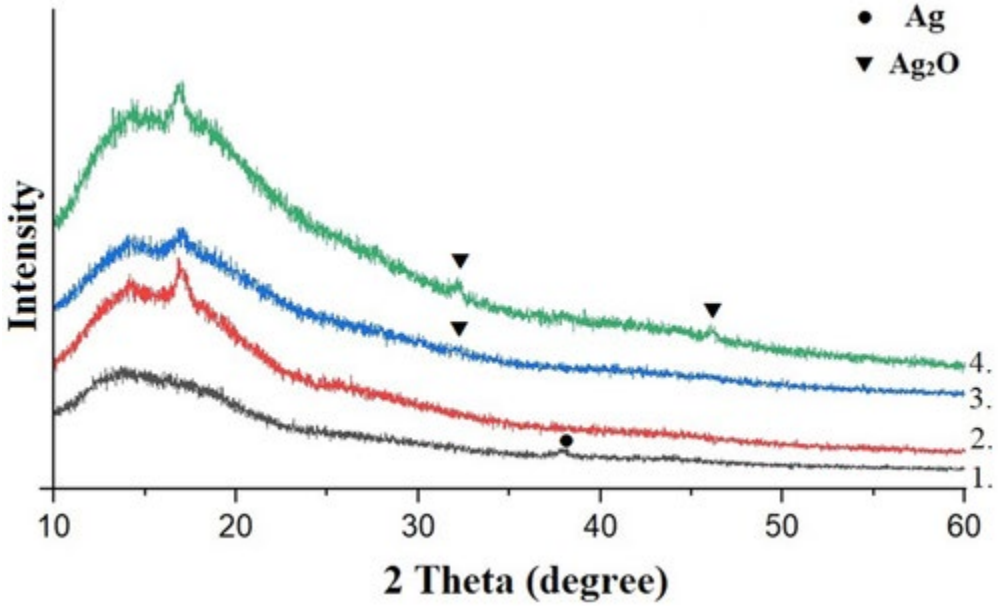

FIGURE 5

Open in figure viewerPowerPoint

XRD pattern of CS20-Ag (1), CS30-Ag (2), CS340-Ag (3), and CS800-Ag (4)

The FTIR spectra of chitosan and CS-Ag NPs are shown in Figure 6. It is worthy to be noted that to analyze the interaction of chitosan macromolecules with the surface of Ag NPs, FTIR spectra

of nanocomposites are often compared with the spectra of neat polymers.[31, 38] However, we consider that this is not really correct approach when the synthesis of nanocomposites was carried out at high temperature. In this case, the observed changes in FTIR spectra associated with chitosan macromolecules transformation during thermal treatment can be falsely identified as related to interaction of chitosan with Ag nanoparticles. Therefore, we compared the FTIR spectra of pristine, heat-treated chitosan and CS-Ag NPs (Figure 6).

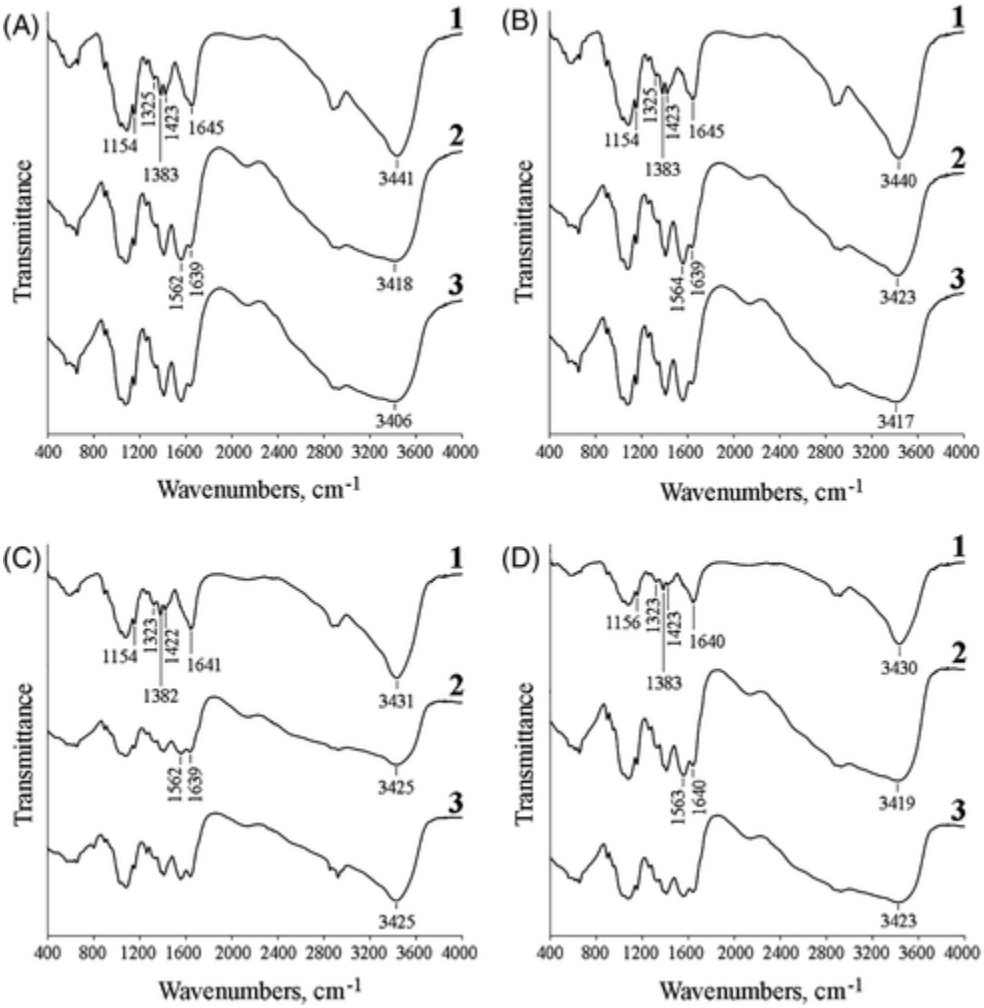

FIGURE 6

Open in figure viewerPowerPoint

FTIR spectra of CS20 (A), CS30 (B), CS340 (C), and CS800 (D) samples. Curves: (1) pristine chitosan, (2) chitosan after 6 h of heating at 95°C and (3) CS-Ag NPs

The FTIR spectra of pristine chitosan (Figure 6) contained the following characteristic bands: the overlapping bands at 1640–1645 and 1610 cm^{-1} correspond to the stretching vibrations of the carbonyl (νC═O) of the amid group of the acetylated units of chitosan (Amid I band) and deformation vibrations δN□H of the primary amine (Amid II band). The bands at around 1423 and 1383 cm^{-1} assigned to the CH_2 bending and CH_3 symmetric deformation, respectively. The band at 1323–1325 cm^{-1} corresponded to the C□N stretching (Amid III band). The peak at 1154–1156 cm^{-1} is due to the asymmetric stretching of the C□O□C bridge. The strong band at 3430–3441 cm^{-1} is the characteristic for absorption of O□H stretching combined with N□H stretching, as well as intramolecular hydrogen bonds. In the FTIR spectra of chitosan samples, treated at 95°C for 6 h under the conditions identical to silver nanoparticle preparation, the significant changes were observed (Figure 6).

For instance, in the case of CS20, the bands at 1645 and 1610 cm^{-1} were shifted to 1639 and 1562 cm^{-1}, respectively. Moreover, the intensity of νC═O band decreased, while the significant growth at 1562 cm^{-1} (δNH) occurred (Figure 6). Therefore, it can be suggested that the deacetylation of chitosan upon heating could be carried out.[56] The band at 1383 cm^{-1} assigned to CH_3 symmetric deformation has almost disappeared, that also confirms the occurrence of deacetylation. The same changes were observed in the spectra of chitosan with different molecular weight (Figure 6B–D).

The FTIR spectra of the obtained nanoparticles were almost identical to the heat-treated chitosan (Figure 6). However, in the spectra of CS20-Ag NPs, the band at 1643 and 1562 cm^{-1}, ascribed to νC═O and δNH, decreased reflecting the presence of interactions between these functional groups of chitosan and silver core (Figure S3). Compared to pristine CS20, in the spectra of heat-treated CS20 and CS20-Ag NPs the peak corresponding to OH and NH stretching became significantly wider and shifted from 3441 cm^{-1} to 3418 and 3406 cm^{-1}, respectively. The widening of the peak at this region and its shifting to short-wavelength indicated the formation of intra- and intermolecular hydrogen bonds.

Silver nanoparticles are of great interest for application in biomedical fields. Despite numerous favorable properties, biomedical prospects of Ag nanoparticles are overshadowed by low stability of bare silver nanoparticles and high-level toxicity.[57] In this regard, the colloidal stability of silver-based nanomaterials is a very important factor, because aggregation may affect their therapeutic properties. In the synthesized CS-Ag NPs, chitosan shell can be responsible for steric and electrostatic stabilization of silver nanoparticles and enhance their colloidal stability. The electrostatic stabilization of the obtained nanocomposites can be evaluated by their zeta-potential values. All obtained samples were positively-charged with zeta-potential values of 26.1–29.5 mV (Table 1), which can determine their aggregative stability due to repulsive forces among the nanoparticles. The ability of chitosan macromolecules to stabilize Ag NPs over time was evaluated during 6 months using UV–Vis, TEM and DLS measurements. In order to evaluate the effect of the storage temperature on the sample stability, CS-Ag NPs were stored in the dark at room temperature (23 ± 2°C) and in a fridge at 4 ± 1°C.

According to the DLS data, there were no significant changes in hydrodynamic diameter of CS20-Ag and CS30-Ag nanocomposites during the time of their storage both at room temperature and in a fridge (Table 2). At the same time, the decrease in hydrodynamic diameter (in approx. two times) upon storage compared to the freshly synthesized samples was observed for CS340-Ag and CS800-Ag NPs (Tables 1 and 2). Such change can be associated with the reorganization of the shell from medium molecular weight chitosan and its compaction. An increase in polydispersity index (up to 0.5–0.6) was detected for CS340-Ag and CS800-Ag stored for 6 months (Table 2). Moreover, it has been also visually observed the partial precipitation of these samples. Thus, after 6 months, the CS340-Ag and CS800-Ag particles suffered the aggregation accompanied by their sedimentation, and only particles with a hydrodynamic diameter of about 1 μm remained in the solution. It should be noted that despite the molecular weight of chitosan, the enhance in zeta-potential value of nanocomposites during storage was observed (Tables 1 and 2).

TABLE 2. Characteristics (DLS data) of the synthesized CS-Ag NPs upon their storage

Sample	d_{mean}, nm	PdI	Zeta potential, mV	d_{mean}, nm	PdI	Zeta potential, mV
	Storage temperature: 4 ± 1°C			Storage temperature: 23 ± 2°C		
1 month						
CS20-Ag	105	0.281	36.0 ± 8.8	110	0.293	36.7 ± 8.7
CS30-Ag	195	0.341	37.6 ± 7.9	200	0.428	38.7 ± 7.4
CS340-Ag	1015	0.210	42.3 ± 7.8	895	0.199	43.5 ± 5.9
CS800-Ag	1160	0.234	43.2 ± 6.7	1275	0.272	42.3 ± 6.0
3 months						
CS20-Ag	115	0.266	33.8 ± 5.2	120	0.283	36.3 ± 5.7
CS30-Ag	180	0.375	35.3 ± 6.1	195	0.384	39.5 ± 7.0
CS340-Ag	1445	0.283	40.8 ± 7.3	690	0.250	43.8 ± 5.5
CS800-Ag	1129	0.157	36.3 ± 6.9	1110	0.226	39.5 ± 6.4
6 months						
CS20-Ag	135	0.398	35.6 ± 8.2	125	0.388	30.3 ± 5.2
CS30-Ag	210	0.424	34.0 ± 5.9	160	0.407	31.3 ± 6.1
CS340-Ag	1065	0.533	34.7 ± 6.0	1125	0.612	36.0 ± 7.2
CS800-Ag	1215	0.507	36.5 ± 6.1	1355	0.544	31.2 ± 5.7

The UV–Vis spectra recorded during storage of nanocomposites are presented in Figure 7. The shape of CS20-Ag NPs spectra registered during its storage remained nearly the same as the initial one and characterized by a single symmetric SPR band (Figure 7A). However, a slight decrease in absorbance value and red shirt of λ_{max} value (from 418 to 424 nm) for CS20-Ag NPs solution during the observation time was observed (Figure 7A). It is well known[58-60] that the wavelength of the SPR band maximum is correlated with size of silver nanoparticles. Thus, according to the UV–Vis data, the mean diameter of the freshly synthesized CS20-Ag was lower in comparison with the stored sample. Another situation was observed for CS30-Ag NPs: an increase (in ~1.3 times) in absorbance for solutions stored at room temperature in the dark was observed. (Figure 7B). The absorbance value enhanced from 0.88 to 1.22 after 1 month of storage and remained stable after 6 months (Figure 7B). This phenomenon can be interpreted by slow additional reduction of silver cations fixed on the chitosan chains. Since CS30-Ag

nanocomposites were stored in the dark, the reduction could only occur under the action of chitosan. It seems the obtained nanocomposite contains some amount of non-reduced silver cations fixed on CS30 chains (in the form of coordination complexes or other species) and during storage they were slowly converted to Ag nanoparticles. These data are in good agreement with literature data indicating the possibility of the generation of new Ag nanoparticles during storage.[22, 61] For CS30-Ag samples stored at (4 ± 1)°C only slight increase in absorbance was observed (Figure 7B). While a small SPR peak was visualized for the freshly synthesized NPs based on medium molecular weight chitosan, it disappeared during storage, and the total absorption of the solutions also decreased which confirmed the aggregation of the particles (Figure 7C,D).

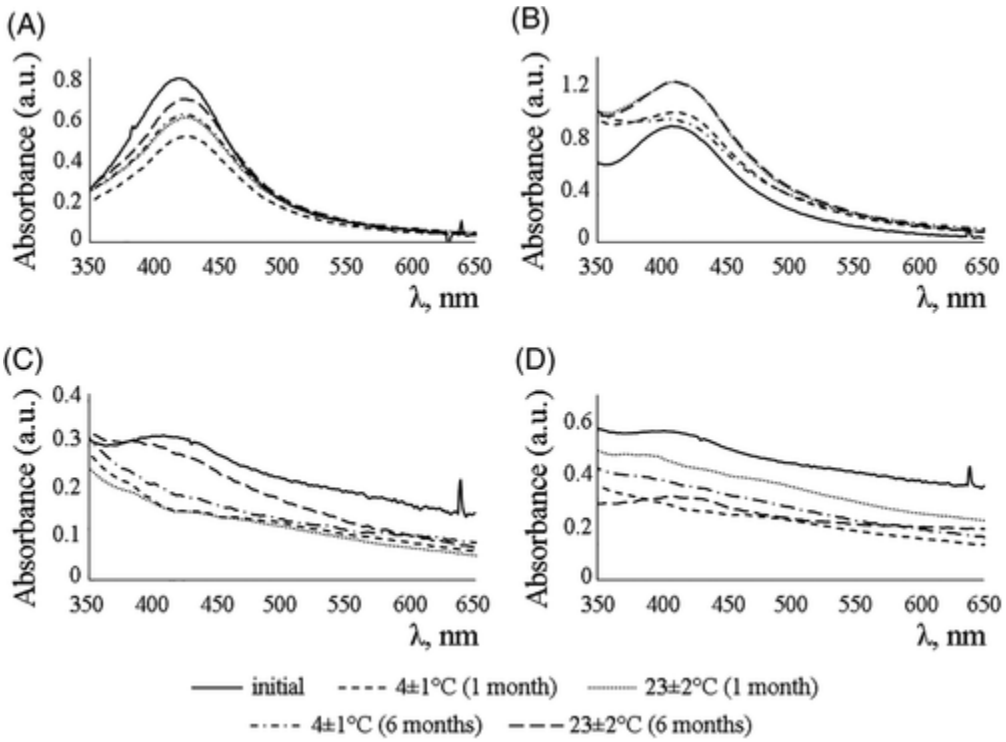

FIGURE 7

Open in figure viewerPowerPoint

UV–Vis absorption spectra measured during storage of CS20-Ag (A), CS30-Ag (B), CS340-Ag (C), and CS800-Ag (D) NPs

The aggregation of particles during storage can be unambiguously confirmed or disproved using TEM. TEM images revealed that the stored samples of CS20-Ag and CS30-Ag NPs were well dispersed and without significant signs of aggregation (Figure 8A,B). Moreover, TEM images of the stored samples of CS20-Ag and CS30-Ag NPs were similar to the freshly synthesized ones, indicating that low molecular weight chitosan can stabilize Ag nanoparticles due to the steric and electrostatic factors (Figures 4A,B and 8A,B). On the contrary, TEM images of CS340-Ag and CS800-Ag showed particle agglomeration (Figure 8C,D). According to the TEM images (Figure 8C,D), medium molecular weight chitosan, apparently, acted as a flocculant promoting particle agglomeration by inter-particle bridging.

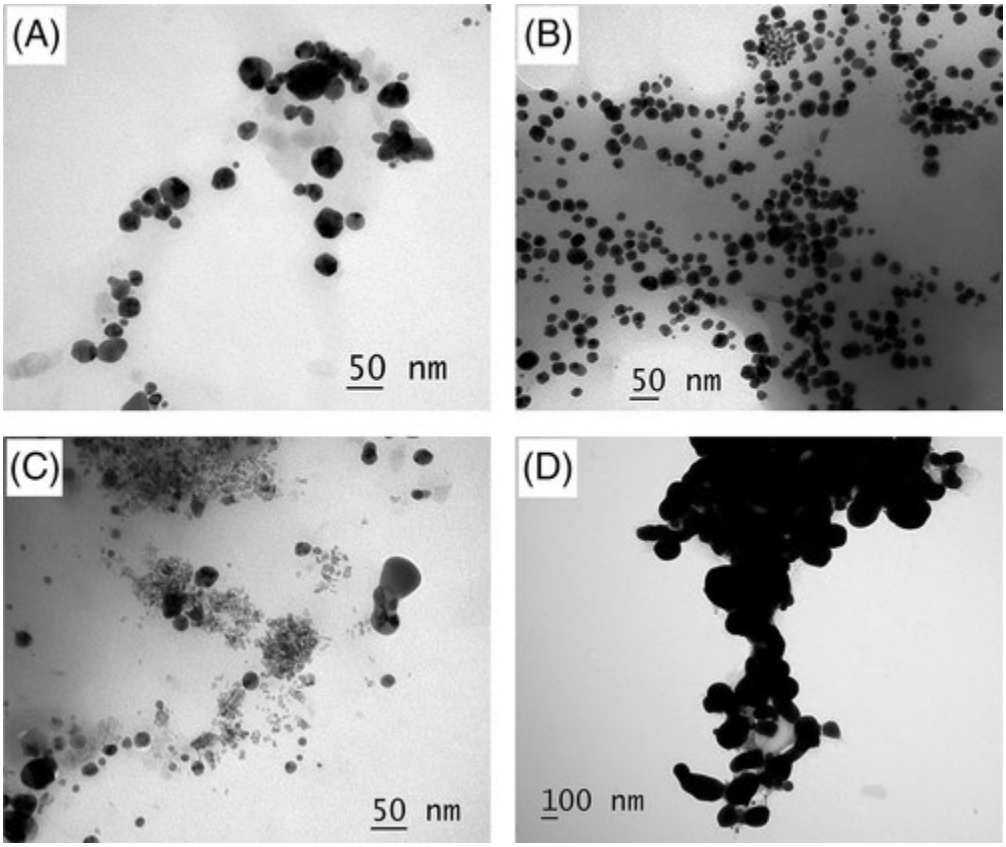

FIGURE 8

Open in figure viewerPowerPoint

TEM images of CS20-Ag (A), CS30-Ag (B), CS340-Ag (C), and CS800-Ag (D) NPs after storage at 23 ± 2°C for 3 months

For further practical application, it is important to evaluate the amount of the released silver cations during storage. According to AAS data, the amount of the released Ag^+ was less than 2.5% for CS20-Ag and CS30-Ag after 1 month, and this parameter was negligibly increased (up to 4%) after 3 months. For CS340-Ag, the amount of the detected free Ag^+ was 3.5% and 4.5% after 1 and 3 months of shelf life, respectively. CS800-Ag was characterized by a huge amount of the released Ag^+: 20.6% of silver cations from nanocomposite were detected in dialysis media after 1 month of storage, while their additional release was only 5% after 3 months. So, the high release of Ag^+ from CS800-Ag sample can be dealt with the lower reducing power of medium molecular weight chitosan and the presence of Ag_2O in the nanocomposite. It has been reported earlier by References [62, 63] that increase in chitosan molecular weight led to the decrease in its reducing power and antioxidant activity. They explain this effect by more compact structure of high molecular weight chitosan due to the greater number of inter- and intramolecular bonding and the restricted chance of exposure of their amine groups.[62, 63] The decrease in the reducing power of chitosan with increase in its molecular weight was also observed in our study. Wei and co-authors demonstrated that the interaction of chitosan with silver nitrate proceeds through the formation of Ag_2O at an intermediate stage which is subsequently reduced by chitosan to Ag NPs.[42] According to the absorption spectra and XRD data of the synthesized NPs, CS800-Ag sample contained significant amount of Ag_2O which was apparently due to its low-reducing ability. Moreover, the presence of Ag_2O in this sample can be responsible for the observed high release of Ag^+ (20.6%) after a month of storage. It is known that silver oxide has higher solubility in water compared to pure Ag NPs and generates a larger amount of silver cations.[64]

It is known that Ag nanoparticles can exhibit synergetic action with essential oils[65] and commercially available antibiotics.[13, 25, 66, 67] Moreover, the combination of Ag NPs with some antibiotics as antibacterial agents is practiced in experimental medicine.[13] Therefore, the ability of the synthesized CS-Ag NPs to enhance the effect of kanamycin and ampicillin was studied. Gram-positive bacteria *Staphylococcus aureus* and gram-negative bacteria *Escherichia coli* were selected for testing antibacterial activity. First, the antibacterial activity of the obtained samples was evaluated. It has been determined that neither initial synthesized CS-Ag NPs exhibited any positive activity against *E. coli* or *S. aureus*. At the same time, concentrated in four times CS-Ag NPs displayed an antimicrobial activity both against *E. coli* or *S. aureus* (Table 3).

TABLE 3. Inhibition zones (mm) of CS-Ag NPs concentrated in four times

Sample	*Escherichia coli*	*Staphylococcus aureus*
CS20-Ag	9	8
CS30-Ag	9	9
CS340-Ag	7	7
CS800-Ag	10	11.5

To study the synergetic antibacterial potential, CS-Ag NPs were added to the antibiotic disks at a concentration in which they do not have their own activity. It is known[68] that chitosan displays antimicrobial activity against both gram-positive and gram-negative bacteria. Therefore, in order to evaluate possible contribution of the proper chitosan in the nanoparticles effect, antibiotic disks with chitosan were used as control samples. It has been established that despite the molecular weight of chitosan, no enhancement in growth inhibition of *E. coli* and *S. aureus* bacteria was observed upon their combination with antibiotics (Table 4). The inhibition zones for all control samples (antibiotic disk+ distilled water or chitosan solution) were identical: 17 and 18 mm against *E. coli* and 18 and 22 mm against *S. aureus* for kanamycin and ampicillin, respectively. At the same time, it has been determined that the antibacterial activity of these antibiotics was enhanced in combination with CS-Ag NPs against both gram-positive and gram-negative bacteria (Table 4). When CS-Ag NPs were added to antibiotic disk, the increase in inhibition area was observed (Table 4). It has been established that CS20-Ag and CS30-Ag NPs showed similar effect against of *E. coli* in combination with kanamycin and ampicillin. Among all the obtained samples, CS800-Ag enhanced the effect of the antibiotics against *E. coli* the most: an increase in fold area was 0.174–0.249. It can be explained by the presence of Ag^+ in this sample, which possess more strong antimicrobial effect compared to Ag nanoparticles.[69] It should be pointed out that synergetic antibacterial effect was more pronounced against gram-negative bacteria compared to gram-positive one (Table 4). The elevated activity of the synthesized nanocomposites against gram-negative bacteria is in good agreement with literature data. It is well known that gram-positive bacteria are more resistant to the action of Ag nanoparticles as compared to gram-negative species, which deals with different thickness and structure of their cell membrane.[2, 10, 48, 70, 71] The observed synergetic effect of the combinations of CS-Ag NPs and antibiotics can be explained as follows. The interaction between CS-Ag NPs and microbial membrane is an important step in the antibacterial activity because membrane is the first main target of the attack. It is considered that electrostatic attraction between negatively charged bacterial cells and positively charged nanomaterials is important for their bactericidal

activity.[47] It seems that the amplification of an antibacterial effect for nanocomposite-antibiotic combinations may be dealt with the strong positive charge of nanocomposite due to the presence of chitosan, since it is known that chitosan binding to the negatively charged bacterial cell wall causes disruption of the cell, as well as it can enhance the effect of antimicrobial agents due to delivery-promoting action.[11, 35, 72] Moreover, one of the possible mechanism of Ag nanoparticles antibacterial action deals with their attachment to the surface of the cell membrane disturbing permeability, integrity and respiration functions of the cell.[9, 10, 12, 13] Thus, altering the membrane permeability under the action of CS-Ag NPs promotes the penetration of antibiotic in the bacterial cell resulting in enhanced antimicrobial effect.

TABLE 4. Inhibition zones (mm) upon adding 30 μg of samples to antibiotic standard disk

Sample	*Escherichia coli*				*Staphylococcus aureus*			
	Kanamycin (standard disk, 30 μg)	**Increase in fold area[a]**	**Ampicillin (standard disk, 10 μg)**	**Increase in fold area[a]**	**Kanamycin (standard disk, 30 μg)**	**Increase in fold area[a]**	**Ampicillin (standard disk, 10 μg)**	**Increase in fold area[a]**
H_2O	17	-	18	-	18	-	22	-
CS20-Ag	18.5	0.184	19	0.114	19	0.114	23	0.093
CS20	17	-	18	-	18	-	22	-
CS30-Ag	18.5	0.184	19.5	0.174	18.5	0.056	24	0.190
CS30	17	-	18	-	18	-	22	-
CS340-Ag	18	0.121	19	0.114	19	0.114	23	0.093
CS340	17	-	18	-	18	-	22	-
CS800-Ag	19	0.249	19.5	0.174	18.5	0.056	23.5	0.141
CS800	17	-	18	-	18	-	22	-

- [a] Fold increases for different nanocomposites were calculated as $(a - a_0)/a_0$, where a and a_0 are the inhibition zones with and without nanocomposite, respectively.

4 CONCLUSIONS

This work has presented the eco-friendly technique to obtain aggregately stable positively charged nanocomposites, containing Ag nanoparticles enclosed within chitosan shell. It has been

demonstrated that chitosan can effectively produce silver nanoparticles and in this reaction it acts both as the reducing and the protective coating-forming agent. A correlating discussion has been given on kinetic regularities of the reaction depending on the molecular weight of the used chitosan. The obtained data showed that the increase in chitosan molecular weight led to the decrease in their reducing ability. Moreover, it has been also found the presence of silver oxide in the samples obtained by the assistance of medium weight chitosan.

The comparative assessment of the long-term stability of the obtained CS-Ag NPs under different temperature has been carried out. Our results showed that among all the synthesized samples, CS20-Ag and CS30-Ag NPs were stable during their long-term storage without significant alterations in their physicochemical properties, while it is better to store them at 4 ± 1°C. It has been proved that molecular weight of chitosan plays a key role in providing stability to silver nanoparticles. Low molecular weight chitosan provides silver nanoparticle stability due to the steric and electrostatic factors. On the contrary, medium molecular weight chitosan acts, apparently, as a flocculant resulting in the particle aggregation and sedimentation upon storage.

The synthesized CS-Ag NPs displayed synergetic action in combination with common antibiotics that opens the prospects for their application to create new effective antibacterial delivery systems.

ACKNOWLEDGMENT

This work was supported by the Belarusian Republican Foundation for Fundamental Research and State Committee on Science and Technology of the Republic of Belarus (Grant X20SRBG-002).

CONFLICT OF INTEREST

The authors have no conflict of interest to declare.